

Synthesis of 1,3-diphenyl-2-propyn-1-ol derivatives in water catalyzed by silver ions immobilized on the magnetic cross-linked chitosan

Fatemeh Rafiee^{*a}, Sahar Kermani^a

a) Department of Organic Chemistry, Faculty of Chemistry, Alzahra University, Tehran, Iran

Received 27 July 2022; received in revised form 12 November 2022; accepted 12 December 2022 (DOI: 10.30495/IJC.2022.1964242.1954)

ABSTRACT

In this work, chitosan biopolymer was cross-linked by starch oxide through the covalent bond formation between amine groups of chitosan and aldehyde functional of oxidized starch. A magnetic bio-support was obtained due to the treatment of the produced hybrid biopolymer with iron oxide nanoparticles. As a result of exposing of silver nitrate salt to magnetic polymer, silver ions (Ag_2O) and also Ag metal nanoparticles were deposited on this bio-support. The silver oxide was decorated on the magnetic chitosan biopolymer could catalyzed the cross-coupling reaction of substituted benzaldehydes with phenylacetylene in the presence of PPh_3 (20 mol%) in water to achieve 1,3-diphenyl-2-propyn-1-ol derivatives in good yields at proper reaction times.

Keywords: Chitosan supported catalysts, Magnetic chitosan, Silver catalyzed coupling reaction, 1,3-diphenyl-2-propyn-1-ol

1. Introduction

Alkynylation of carbonyl compounds has been recognized as an interesting methodology for the synthesis of the corresponding propargylic alcohols [1]. These valuable compounds are utilized as useful intermediates for the synthesis of many oxygens and also nitrogen-containing heterocycles due to the reaction of propargyl alcohols with amines [2]. Two-step process of preparation of metal acetylide with the use of stoichiometric amounts of metal reagents such as organolithium [3] and dialkylzinc [4-5] and then nucleophilic additions to carbonyl compounds, moisture sensitivity and low tolerance of functional groups are as limiting factors in traditional methods. The in situ generations of metal alkynides and subsequently addition to aldehydes has developed as an efficient chemical selective and atom-economical approach for the synthesis of propargyl alcohols. The catalytic C-H activation of terminal alkynes and aldehyde-alkyne coupling reaction catalyzed by various homogeneous

transition metal salts with or without ligands such as $\text{InBr}_3/\text{BINOL}$ [6], $\text{InBr}_3\text{-Et}_3\text{N}$ [7], $\text{InBr}_3\text{-i-Pr}_2\text{NEt}$ [8], $\text{RuCl}_3\text{-In(OAc)}_3$ [9] and $\text{AgCl/Cy}_3\text{P}$ [10].

Chitosan is an amino polysaccharide having D-glucosamine and N-acetyl-D-glucosamine units. The renewability, biodegradability, biocompatibility, interchangeable functionality, physical and chemical modification possibility due to the availability of NH_2 and OH functional characteristics and excellent adsorption capability make it as a practical candidate in various fields. The various reports in the literature focused on the multiple roles of this valuable biopolymer in organic synthesis as an organocatalyst [11], as a capping macroligand for metal ions uptake [12], synthesis and stabilization of metal nanoparticles [13-14], water purification [15], food packaging [16], therapeutic supplements and biomedical applications especially as a non-toxic support for drug delivery [17] and also enzyme immobilization [18].

Immobilization of catalytic metals on solid supports having chelating functional groups could significantly enhance catalyst availability and recovery. In this line, various metallic species such as palladium, copper, silver, gold, and rhodium were immobilized on chitosan bio support and showed catalytic activity in the metal-

^{*}Corresponding author:

E-mail address: f.rafiie@alzahra.ac.ir (F. Rafiee)

catalyzed organic reactions [19]. Silver-chitosan nanocomposites have shown antifungal and antibacterial properties. The catalytic activity Ag-coated on the magnetic chitosan hybrid was examined in the reduction of environmentally hazardous dyes [20] and nitroarene pollutants like 4-nitrophenol [21-23]. Han and coworkers in 2020 synthesized Ag NP adorned chitosan-alginate dual bio-polysaccharide and investigated its human lung protective effects against α -Guttiferin and also its efficiency in one-pot multicomponent synthesis of biologically potent 2H-indazolo[2,1-b]phthalazine-trione derivatives [24]. Silver nanoparticles decorated magnetic-chitosan microsphere were applied for efficient removal of dyes and microbial contaminants [25].

Using of the magnetic nanoparticles with high stability and ready availability could effectively improve the loading and catalytic efficiency of immobilized catalysts due to the high surface-to-volume ratio and also quick magnetic separation [26-33]. In continuation of our research in the synthesis of bionanocomposites based on chitosan [18-19, 34-36], in here we cross-linked chitosan with starch dialdehyde for the enhancement of the mechanical strength and chemical resistance and then prepared a magnetic biopolymer hybrid due to the treatment of cross-linked polymer and Fe_3O_4 nanoparticles. The final nanocomposite was resulted by the decoration of silver ions on the magnetic biosupport based on chitosan.

2. Experimental

Preparation of $\text{Fe}_3\text{O}_4/\text{CS-St}/\text{Ag}^+$ nanocomposite

The magnetically magnetic modified biopolymer ($\text{Fe}_3\text{O}_4/\text{CS-St}$) was prepared according to the procedure that described in our previous work [28]. (Starch procured from Merck company as starch soluble GR for analysis ISO and Chitosan with medium molecular weight and 75-85% deacetylated degree purchased from Sigma-Aldrich). Starch biopolymer (1.5 g) was oxidized with sodium periodate solution (0.3 M/L, 50 mL) at 30 °C under stirring in dark conditions for 2h. Then, ethylene glycol solution (0.1 M/L, 10 mL) was added to remove the remaining iodate. The obtained oxidized starch was filtrated and purified by precipitation with acetone. For the bio-crosslinking of chitosan, oxidized starch (0.5 g) was added to the acidic chitosan solution (1 g in 50 mL acetic acid solution (2% v/v)) and stirred at room temperature for 3 h. Then, the formed hydrogel was cast casted into a glass Petri petri plate and dried at room temperature under a vaccum vacuum. For the magnetization of the cross-linked biopolymer, Fe_3O_4 NPs (1.5 g) that were obtained through the co-

precipitation process of $\text{FeCl}_2 \cdot 4\text{H}_2\text{O}$ and $\text{FeCl}_3 \cdot 6\text{H}_2\text{O}$ at a 1:2 ratio were added to the solution of CS-St polymer (2 g) in acetic acid (40 mL, 2 wt%) and sonicated and stirred for 2 h at room temperature. The magnetic biosupport ($\text{Fe}_3\text{O}_4/\text{CS-St}$) was separated using of an external magnet, washed with ethanol and deionized water several times, and dried under vaccum at 50 °C.

In the next step, for the silver decoration on the magnetic biosupport, a solution of AgNO_3 (0.7 g, in 25 mL H_2O) was added to $\text{Fe}_3\text{O}_4/\text{CS-St}$ (1.5 g) under sonication conditions for 1h and stirred at room temperature for 12 h. The final composite ($\text{Fe}_3\text{O}_4/\text{CS-St}/\text{Ag}^+$) was separated magnetically and washed with ethanol and deionized water, then dried in room temperature.

The synthesis of 1,3-diphenyl-2-propyn-1-ol derivatives by $\text{Fe}_3\text{O}_4/\text{CS-St}/\text{Ag}^+$

Benzaldehyde derivative (0.25 mmol), phenylacetylene (0.4 mmol), diisopropyl ethylamine (0.1 mmol), $\text{Fe}_3\text{O}_4/\text{CS-St}/\text{Ag}^+$ nanocomposite (0.003 g), PPh_3 (0.05 mmol) and water (3 mL) were added to a round bottom balloon and stirred at 60 °C. The propargyl alcohol product formation was examined by TLC (*n*-hexane/EtOAc, 9:1) and GC using *n*-hexane as an external standard. After the complete reaction, the mixture was cooled at room temperature, the mixture was diluted with distilled water and *n*-hexane, and the nanocatalyst was removed by an external magnet. Then, the organic layer was extracted and dried over Na_2SO_4 . The residue was purified by silica gel column chromatography (*n*-hexane: EtOAc, 9:1).

1-(4-Bromophenyl)-3-phenylprop-2-yn-1-ol: Yellow oil, FT-IR (cm^{-1}): 3419 (O-H stretching vibrations), 3030 (C-H Aromatic stretching vibrations), 2197 (C=C stretching vibrations), 1642 and 1487 (C=C Aromatic stretching vibrations), 1463 (O-H bending vibrations), 1170 (C-O stretching vibrations), 960 (=C-H in-plane bending vibrations) and 756 cm^{-1} (C-Br stretching vibrations), MS: 287 (M^+ [$\text{C}_{15}\text{H}_{11}\text{OBr}$]), $\text{M}+2$ (289), 207 (M-Br).

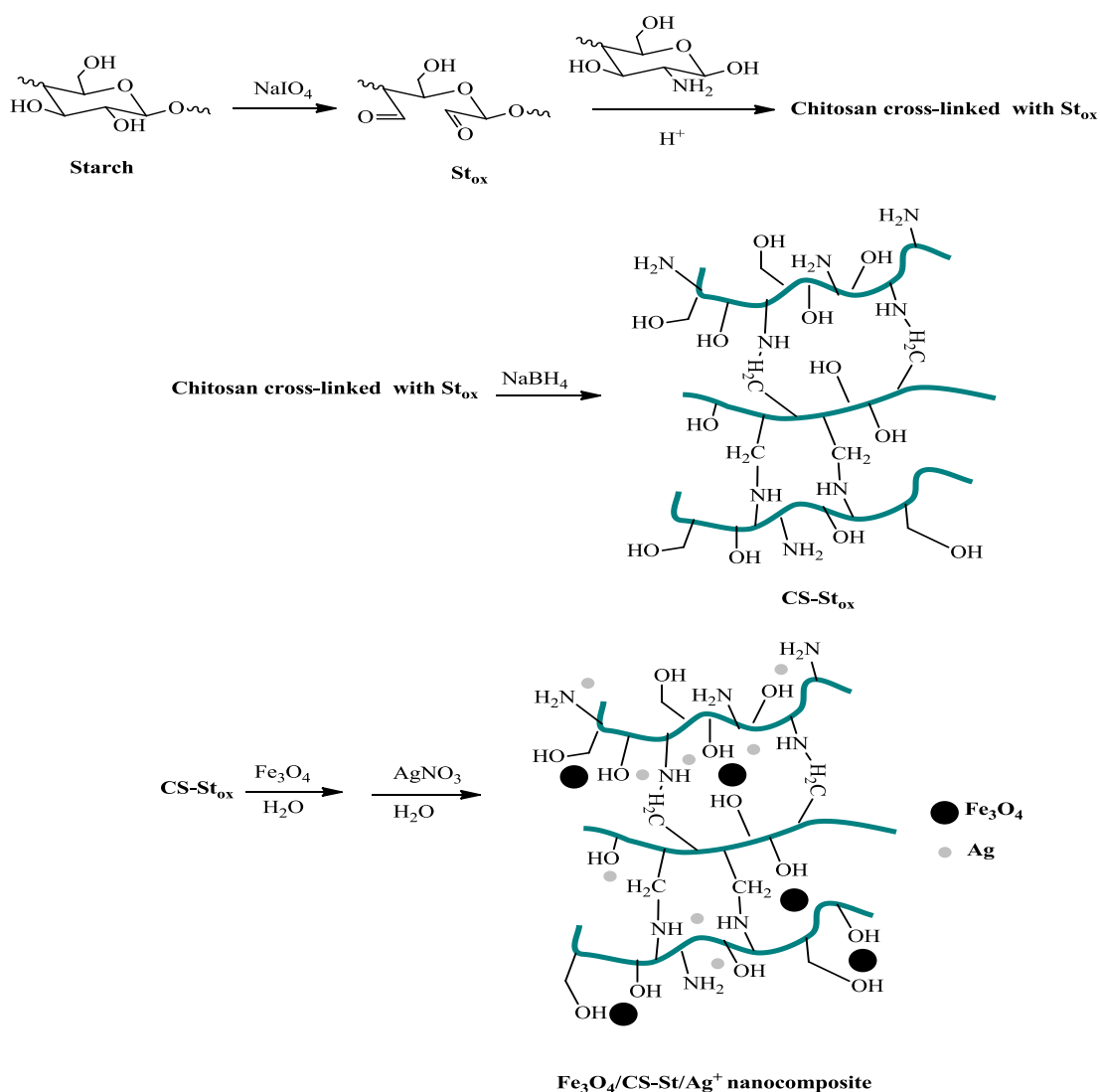
1-(4-Methoxyphenyl)-3-phenylprop-2-yn-1-ol: FT-IR (cm^{-1}): 3394 (O-H stretching vibrations), 3030 (C-H Aromatic stretching vibrations), 2928-2840 (C-H (OMe) stretching vibrations) 2198 (C=C stretching vibrations), 1663 and 1461 (C=C Aromatic stretching vibrations), 1444 (O-H bending vibrations), 1421 (C-H bending vibrations), 1167 (C-O stretching vibrations), MS: 238 (M^+ [$\text{C}_{16}\text{H}_{14}\text{O}_2$]), 221 (M-OH), 207 (M-OMe) 178 (M - (CHO and OMe)).

3. Results and Discussion

Preparation and characterization of $Fe_3O_4/CS-St/Ag^+$ nanocomposite

The periodate oxidation process was applied for the preparation of dialdehyde starch from starch as a green macro molecule cross-linked agent. The amine groups of chitosan were reacted with aldehyde functional of oxidized starch. Reduction with $NaBH_4$ converted imine bonds to the saturated C-N bonds. After the magnetization process of oxidized starch-chitosan hybrid with iron oxide nanoparticles, treatment of magnetic support with an aqueous solution of silver nitrate led to Ag-adorned chitosan composite formation (Scheme 1).

The magnetic cross-linked chitosan biopolymer was prepared and characterized according to our previous work [28] and inhere silver oxide (Ag_2O) was decorated on its surface. FT-IR spectra of the step-by-step synthesized $Fe_3O_4/CS-St/Ag^+$ nanocomposite was shown in Fig. 1. In the FT-IR spectra of $Fe_3O_4/CS-St/Ag^+$ nanocomposite (Fig. 1) vibrational frequencies of metal-oxygen bond (Ag-O) were observed at around 450 and 800 cm^{-1} [37], Fe-O peak at 585, the skeletal vibration of saccharide structure at 892, the stretching vibrations of C-N and C-O bonds at 1160 and 1089, respectively, C-H stretching vibrations at 2925 and bending at 1382, secondary N-H bending at 1521, and O-H and N-H stretching vibrations at 3420 cm^{-1} . FT-IR characteristic absorption of $Fe_3O_4/CS-St/Ag^+$ are given in Table 1.



Scheme 1. The preparation of $Fe_3O_4/CS-St/Ag^+$ nanocomposite

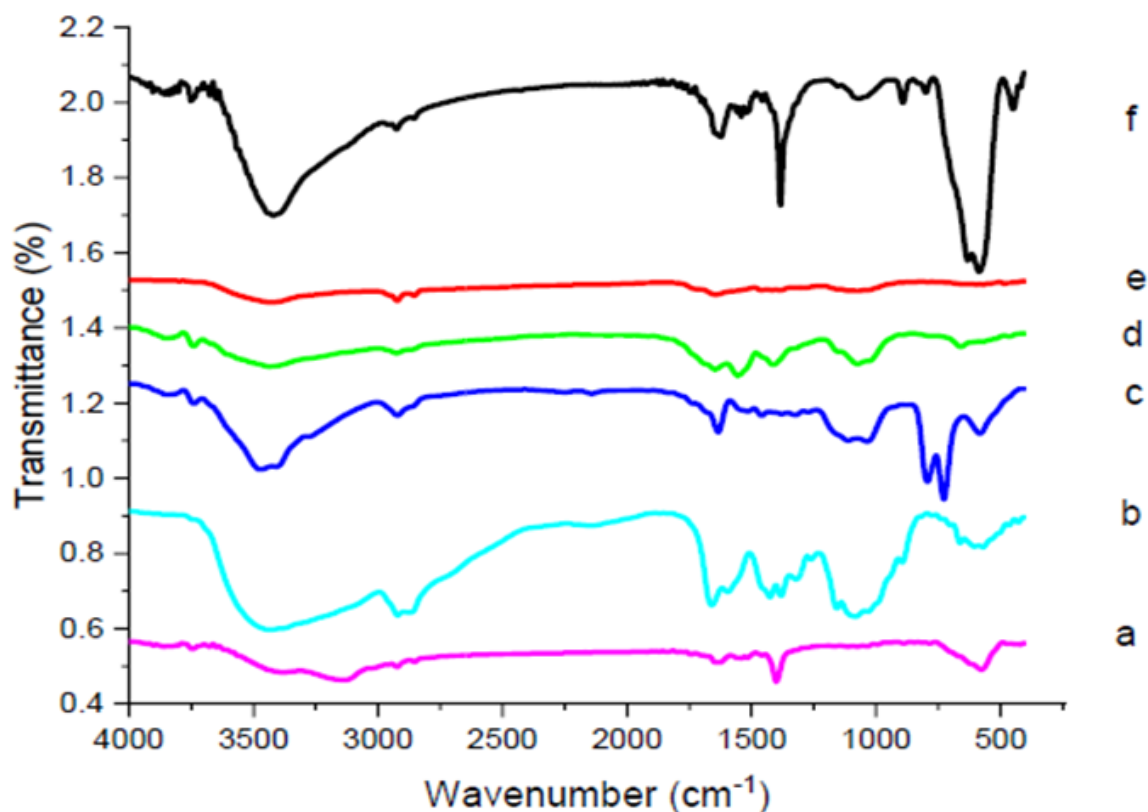


Fig. 1. FT-IR spectra, a: Fe_3O_4 , b: chitosan (CS), c: starch oxide (St_{OX}), d: CS- St_{OX} with imine bonds, e: CS- St_{OX} with amine bonds, f: $\text{Fe}_3\text{O}_4/\text{CS-St}/\text{Ag}^+$ nanocomposite

Table 1. FT-IR characteristic absorption of $\text{Fe}_3\text{O}_4/\text{CS-St}/\text{Ag}^+$

Entry	Functional group	Absorption(cm^{-1})	Ref
1	N-H and O-H stretching vibrations	3420	[28]
2	C-H stretching vibrations	2925	[28]
3	C-H bending vibrations	1382	[28]
4	secondary N-H bending	1521	[28]
5	C-N stretching vibrations	1160	[28]
6	C-O stretching vibrations	1089	[28]
7	The skeletal vibration of saccharide structure	892	[28]
8	Fe-O	585	[28]
9	Ag-O stretching vibrations	450 and 800	[37]

The powder XRD plan of the $\text{Fe}_3\text{O}_4/\text{CS-St}/\text{Ag}^+$ nanocomposites are presented in **Fig. 2**. The diffraction peaks of Fe_3O_4 nanoparticles with cubic spinel structure are appeared at $2\theta = 30.98, 35.48, 43.26, 53.30, 57.40$ and 62.80° correspond to the crystalline planes (220), (311), (400), (422), (511) and (440) respectively. The additional peaks at $46.20, 67.20,$ and 76.44° are related to the (200), (220) and (311) crystalline planes of Ag

nanoparticles with face-centered cubic (fcc) structure, proposing the amount of silver ions were reduced to metallic silver nanoparticles. Also, the observed diffraction peaks at $2\theta = 27.64, 32.16^\circ$ and $38.12, 54.6, 64.5, 68.7$ are according to the (110), (111), (200), (220), (311) and (222) crystalline planes of silver oxide (Ag_2O) nanoparticles [29].

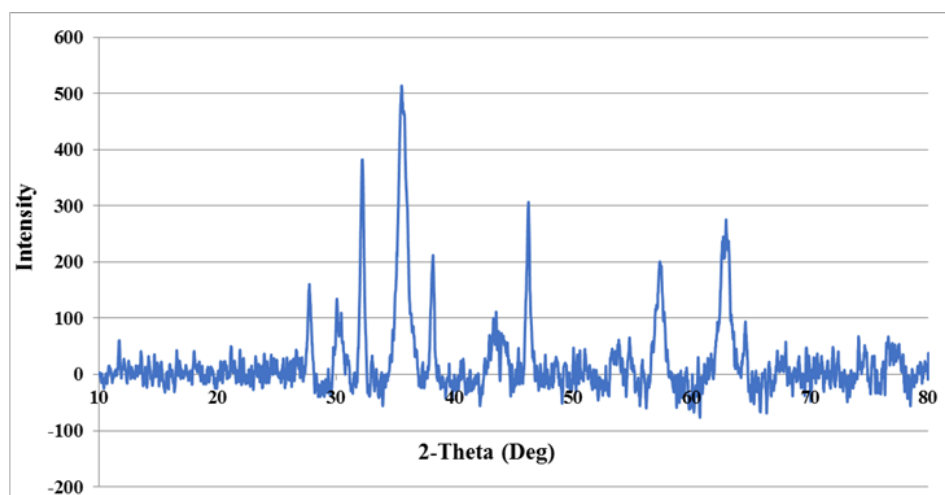


Fig. 2. The powder XRD pattern of the $\text{Fe}_3\text{O}_4/\text{CS-St}/\text{Ag}^+$ nanocomposite

The elemental composition of $\text{Fe}_3\text{O}_4/\text{CS-St}/\text{Ag}^+$ nanocomposites in energy-dispersive X-ray analysis (C, N, O, Fe and Ag) (**Fig. 3**) emphasizes its successful synthesis contain magnetization (Fe and O), polymeric hybrid network (C, N and O) and silver ion immobilization (Ag).

The morphology of $\text{Fe}_3\text{O}_4/\text{CS-St}/\text{Ag}^+$ nanocomposite was examined by using of field-emission scanning electron microscopy (FE-SEM). The results showed that the nanoparticles are spherical and the average particle size is less than 25 nm in diameter (**Fig. 4**).

The saturation magnetization (M_s) of $\text{Fe}_3\text{O}_4/\text{CS-St}/\text{Ag}^+$ nanocomposite resulted in was resulted 39.3 emu g^{-1} that was lower than of M_s of Fe_3O_4 NPs (57 emu g^{-1}) due to the non-magnetic coating (polymer support and silver ions) at the surface of a magnetic core (**Fig. 5**). The nanocatalyst was easily separated from the reaction mixture using an external magnet.

The evaluation of the activity of $\text{Fe}_3\text{O}_4/\text{CS-St}/\text{Ag}^+$ nanocomposite in the synthesis of 1,3-diphenyl-2-propyn-1-ol derivatives

The effect of reaction parameters including solvent, temperature, amount of alkyne substrate, and catalyst was evaluated on the development of the cross coupling reaction of 4-bromobenzaldehyde with phenylacetylene (**Table 2**). The reaction did not progress in the absence of phosphine and catalyst. Phosphine ligand as an electron-donating ligand could be increased the electron density of silver, thus leading led to a weakening of the silver carbon bond and facilitating facilitate its nucleophilic additions to carbonyl groups [10].

We also compared the efficiency of the $\text{Fe}_3\text{O}_4/\text{CS-St}/\text{Ag}^0$ nanocomposite that was prepared via the reduction of Ag^+ ions decorated on the magnetic biopolymer. The results have shown that silver ions catalyzed this coupling reaction through C-H activation of phenylacetylene and metallic nanoparticles have little effect.

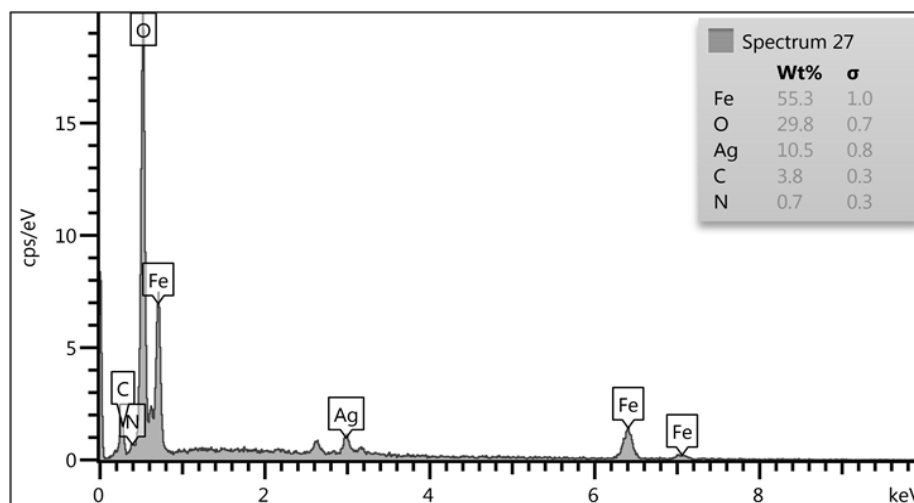


Fig. 3. EDX analysis of $\text{Fe}_3\text{O}_4/\text{CS-St}/\text{Ag}^+$ nanocomposite

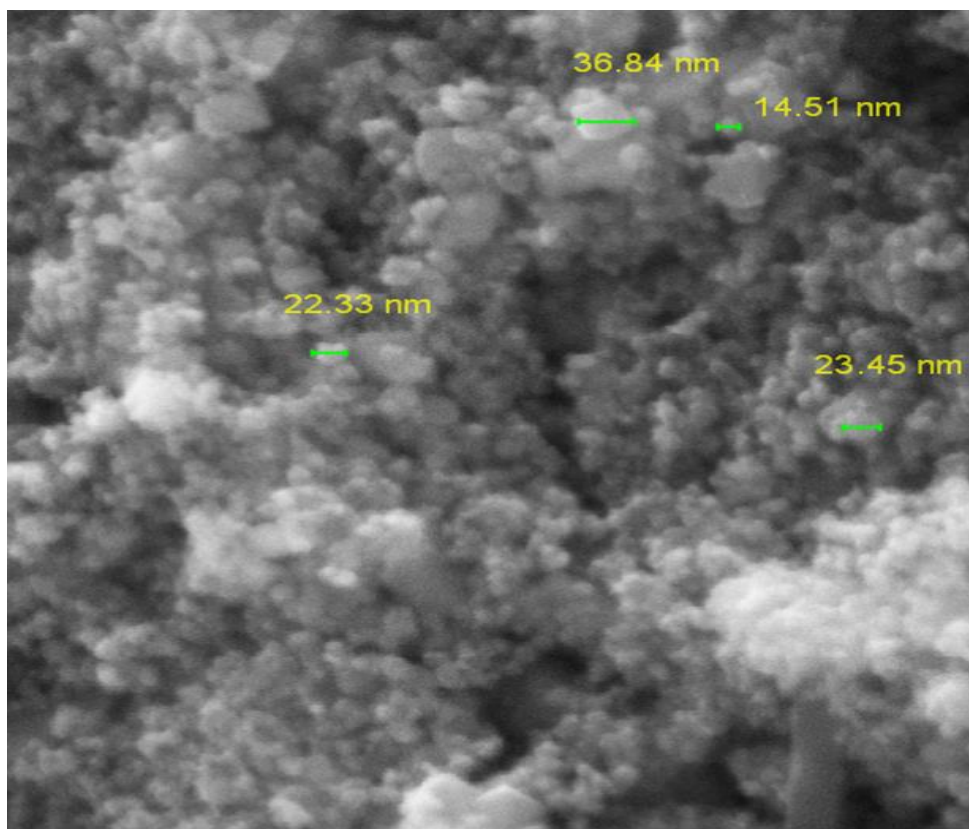


Fig. 4. FE-SEM image of $\text{Fe}_3\text{O}_4/\text{CS-St}/\text{Ag}^+$ nanocomposite

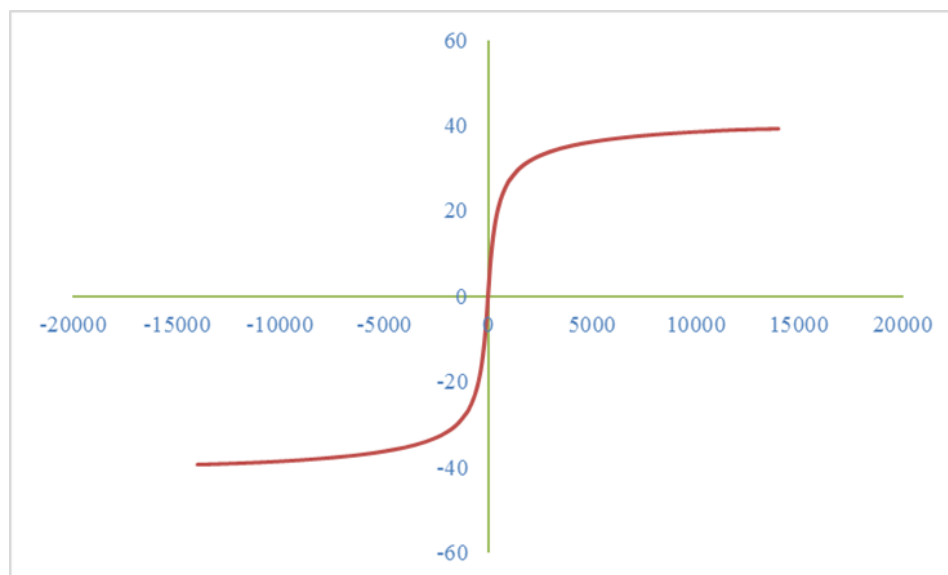
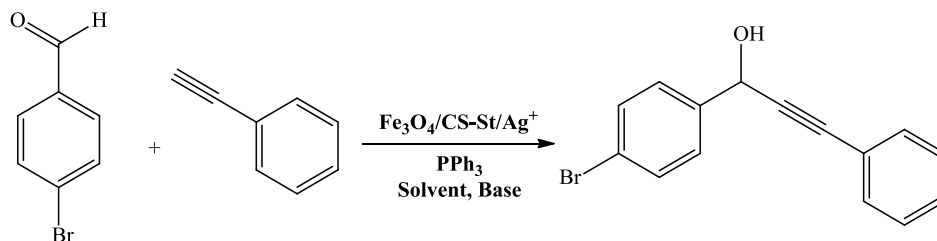


Fig. 5. The VSM curve of $\text{Fe}_3\text{O}_4/\text{CS-St}/\text{Ag}^+$ nanocomposite

The results of the cross coupling of various benzaldehydes with phenylacetylene were detailed in **Table 3**. Benzaldehydes having electron-withdrawing and donating substituents gave the corresponding 1,3-diphenyl-2-propyn-1-ol derivatives in good yields at proper reaction time. However, the higher yields were obtained with electron-withdrawing substituted

benzaldehydes. The Reaction of acetaldehyde as an aliphatic aldehyde was performed under optimal conditions but no alkynylated product was formed. According to literature data, in enolizable aliphatic aldehydes, the abstraction of α -hydrogen and aldol condensation as a side reaction proceeds faster than the nucleophilic addition metal-alkynide intermediate [7].

Table 2. Optimization of conditions of cross coupling reaction of 4-bromobenzaldehyde with phenylacetylene^a

Entry	Solvent	Tem. (°C)	Base	Cat. (g)	Conversion (%)
1	H ₂ O	reflux	i-pr ₂ NEt	0.003	40
2	H ₂ O	60	i-pr ₂ NEt	0.003	85
3	-	60	i-pr ₂ NEt	0.003	-
4	H ₂ O	60	Et ₃ N	0.003	50
5	H ₂ O	60	i-pr ₂ NEt	0.002	60
6	H ₂ O	60	i-pr ₂ NEt	0.004	85
7	H ₂ O	rt	i-pr ₂ NEt	0.003	35
8	H ₂ O	60	K ₂ CO ₃	0.003	20
9 ^b	H ₂ O	60	i-pr ₂ NEt	0.003	-
10	H ₂ O	60	i-pr ₂ NEt	-	-
11 ^c	H ₂ O	60	i-pr ₂ NEt	0.003	Trace
12 ^d	EtOH	60	Et ₃ N	0.005	30
13 ^e	H ₂ O	60	i-pr ₂ NEt	0.003	75

^aReaction conditions: 4-Bromobenzaldehyde (0.25 mmol), phenylacetylene (0.4 mmol), Base (0.1 mmol), PPh₃ (0.05 mmol), nanocomposites (g), Solvent, 1 h, N₂

^bIn the absence of PPh₃

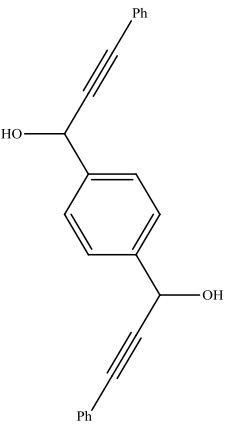
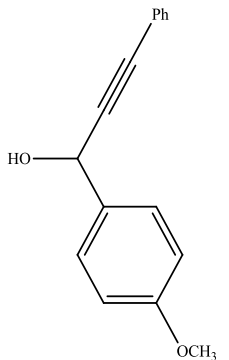
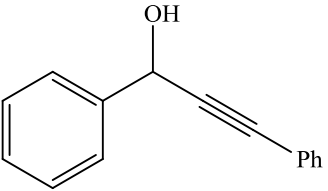
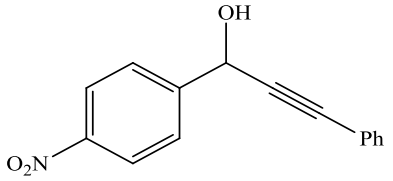
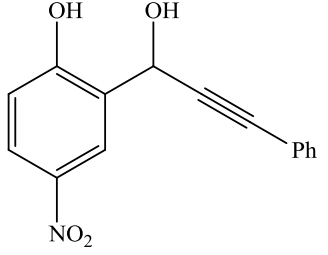
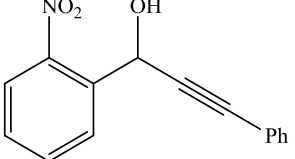
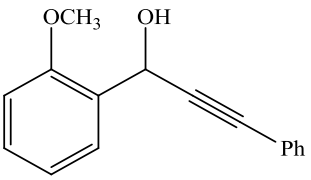
Fe₃O₄/CS-St/Ag⁰ nanocomposites were used as a catalyst

^dAgNO₃ was used as a catalyst

^ePhenylacetylene (0.3 mmol)

Table 3. Cross-coupling of benzaldehydes with phenylacetylene catalyzed by Fe₃O₄/CS-St/Ag⁺ nanocomposite

Entry	PhCHO	Product	Time(h)	Conversion (%)	TON	TOF
1	4-Cl-Ph-CHO		1	95	86.4	86.4
2	4-Br-Ph-CHO		1	85	77.3	77.3
3	3-NO ₂ -Ph-CHO		2	80	72.7	36.3

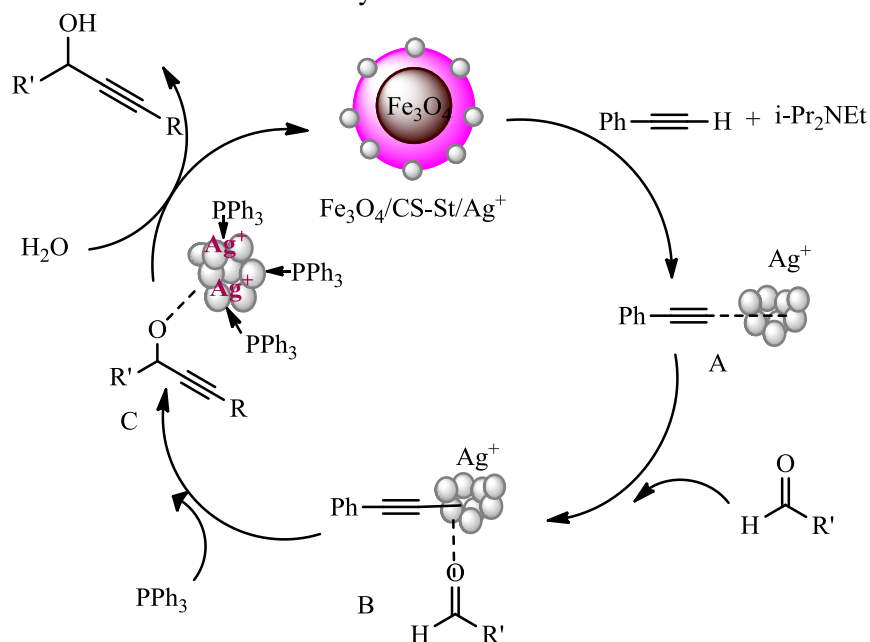
4 ^b	OHC-Ph-CHO		3	80	72.7	24.2
5	4-OMe-Ph-CHO		5	80	72.7	14.5
6	Ph-CHO		3	60	54.5	18.2
7	4-NO ₂ -Ph-CHO		1	90	81.8	81.8
8	4-NO ₂ -Ph-CHO-2-OH		3	80	72.7	24.2
9	2-NO ₂ -Ph-CHO		3	85	77.3	25.8
10	2-OMe-Ph-CHO		3	50	45.4	15.1

11	4-OMe-Ph-CHO-2-OH		3	60	54.5	18.2
12	4-N(Me) ₂ -Ph-CHO		3	70	63.3	21.1
13	CH ₃ -CHO		5	-	-	-

^aReaction conditions: Benzaldehyde (0.25 mmol), Phenylacetylene (0.4 mmol), *i*-pr₂NEt (0.1 mmol), PPh₃ (0.05 mmol, 20 mol%), Fe₃O₄/CS-St/Ag⁺ nanocomposite (0.003 g, 1.1 mol%), H₂O, 60 °C, N₂. ^bBenzaldehyde: phenylacetylene (0.25:0.8)

In this coupling reaction, phenylacetylene is converted to silver alkynide in the presence of diisopropyl ethylamine base and silver catalyst. The generated silver alkynide reagent is stable and has little tendency to

nucleophilic addition to carbonyl functional. Therefore, the coordination of the electron donor phosphine ligand weakens this bond and increases its activity (**Scheme 2**).



Scheme 2. The proposed mechanism for Ag-catalyzed cross-coupling aldehydes with phenylacetylene

The recovery and reusability of $\text{Fe}_3\text{O}_4/\text{CS-St}/\text{Ag}^+$ nanocomposite was examined in the cross coupling of 4-chlorobenzaldehyde and phenylacetylene. At the end of each cycle, the magnetic nanocatalyst was removed using an external magnet, washed with EtOH and water, dried, and reused for the next cycle. The $\text{Fe}_3\text{O}_4/\text{CS-St}/\text{Ag}^+$ nanocomposite was exhibited the same original activity for at least five consecutive times.

To prove the lack of leaching process and the absence of homogeneous catalytic species in the reaction mixture, a hot filtration test was done. The optimized amount of $\text{Fe}_3\text{O}_4/\text{CS-St}/\text{Ag}^+$ nanocatalyst in 2 mL of H_2O as solvent was heated at 60 °C for 1h. Then, the magnetic nanocatalyst was removed from the hot mixture, and reactants, base and PPh_3 were added to the solution and stirred for 2h. The propargyl alcohol product formation was not observed even in longer times. No reaction progress indicates that the catalytic system is heterogeneous.

The catalytic activity of $\text{Fe}_3\text{O}_4/\text{CS-St}/\text{Ag}^+$ nanocatalyst was compared to other catalysts in the cross-coupling of 4-chloro benzaldehyde with phenylacetylene (**Table 4**). The results were demonstrated that the present methodology produced the propargylic alcohol product in a higher yield at a shorter reaction time and allowed for easy magnetic separation of the catalyst.

4. Conclusions

In this work, a chitosan- based magnetic support was prepared for the immobilization of silver ions as Ag_2O . A diverse range of 3-diphenyl-2-propyn-1-ol derivatives were obtained by the cross coupling reaction of various substituted benzaldehydes with phenylacetylene in water as a green solvent in the presence of low loading of the $\text{Fe}_3\text{O}_4/\text{CS-St}/\text{Ag}^+$ nanocomposite in good yields at short reaction times.

High activity, fast and simple separation, and reusability without a gradual decrease in activity are the advantages of this catalytic system. This catalytic system was readily separated by an external magnet and reused for five cycles while maintaining its original activity.

Acknowledgements

We thank the partial financial support received from the research council of Alzahra University.

Conflict of interest

There are no conflicts of interest to declare.

References

- [1] P.G. Cozzi, R. Hilgraf, N. Zimmermann, *Eur. J. Org. Chem.* 2004 (2004) 4095-4105.
- [2] R. Hua, T. A. Nizami, *Org. Chem.* 15 (2018) 198-207.
- [3] S. Kotani, K. Kukita, K. Tanaka, T. Ichibakase, M. Nakajima, *J. Org. Chem.* 79 (2014) 4817-4825.
- [4] L. Pu, *Tetrahedron* 59 (2003) 9873-9886.
- [5] C. Chen, L. Hong, Z.-Q. Xu, L. Liu, R. Wang, *Org. Lett.* 8 (2006) 2277-2280.
- [6] R. Takita, K. Yakura, T. Ohshima, M. Shibasaki, *J. Am. Chem. Soc.* 127 (2005) 13760-13761.
- [7] N. Sakai, R. Kanada, M. Hirasawa, T. Konakahara, *Tetrahedron* 61 (2005) 9298-9304.
- [8] R. Takita, Y. Fukuta, R. Tsuji, T. Ohshima, M. Shibasaki, *Org. Lett.* 7 (2005) 1363-1366.
- [9] C. Wei, C.J. Li, *Green Chem.* 4 (2002) 39-41.

Table 4. The cross coupling of 4-chloro-benzaldehyde with phenylacetylene by various catalytic systems

Entry	Catalyst	Solvent	Temp.(°C)	Time(h)	Yield	Reference
1	ZnEt_2 L (20 mol%), $\text{Ti}(\text{O}^i\text{Pr})_4$	Hexane/ CH_2Cl_2	rt	6	83	[38]
2	Me_2Zn L (0.054 mmol)	Toluene	rt	18	61	[39]
3	ZnEt_2 L (20 mol%), $\text{Ti}(\text{O}^i\text{Pr})_4$	CH_2Cl_2	rt	12	84	[40]
4	ZnEt_2 Silica immobilized L (20 mol%), $\text{Ti}(\text{O}^i\text{Pr})_4$	Toluene	rt	18	84	[41]
5	ZnEt_2 $\text{Ti}(\text{O}^i\text{Pr})_4+(\text{S})\text{-Boc-proline}$ (30 mol%)	Ether, Toluene	rt	12	68	[42]
6	$\text{Cy}_3\text{P}(\text{AgCl})$ (5mol%)	H_2O	80	12	85	[10]
7	$\text{Fe}_3\text{O}_4/\text{CS-St}/\text{Ag}^+$ (0/003 g), PPh_3 (0.05 mmol)	H_2O	60	1	95	This work

- [10] X. Yao, C.J. Li, *Org. Lett.* 7 (2005) 4395-4398.
- [11] A. El Kadib, *ChemsSusChem* 8 (2015) 217-244.
- [12] N.H. Azeman, N. Arsad, A.A.A. Bakar, *Sensors (Basel)* 20 (2020) 3924.
- [13] M. Ottonelli, S. Zappia, A. Demartini, M. Alloisio, *Nanomaterials (Basel)*. 10 (2020) 224.
- [14] T.T.V. Phan, D.T. Phan, X.T. Cao, T.-C. Huynh, J. Oh, *Nanomaterials* 11 (2021) 273.
- [15] A. Spoială, C.I. Ilie, D. Ficai, A. Ficai, E. Andronescu, *Materials* 14 (2021) 2091.
- [16] P. Cazón, M. Vázquez, Applications of chitosan as food packaging materials. In: Crini G., Lichtfouse E. (eds) *Sustainable Agriculture Reviews 36. Sustainable Agriculture Reviews*, 36 (2019) 81-123.
- [17] R. Parhi, *Environ Chem. Lett.* 18 (2020) 577-594.
- [18] F. Rafiee, M. Rezaee, *Int. J. Biol. Macromol.* 179 (2021) 170-195.
- [19] F. Rafiee, *Curr. Org. Chem.* 23 (2019) 390-408
- [20] M. Kaloti, A. Kumar, *ACS Omega.* 3 (2018) 1529-1545.
- [21] K. Hasan, I.A. Shehadi, N.D. Al-Bab, A. Elgamouz, *Catalysts* 9 (2019) 839.
- [22] I. Sargin, *Int. J. Biol. Macromol.* 137 (2019) 576-582.
- [23] R. Taheri-Ledari, S.S. Mirmohammadi, K. Valadi, A. Maleki, A.E. Shalan, *RSC Adv.* 10 (2020) 43670-43681.
- [24] Y. Han, Y. Gao, X. Cao, M.M. Zangeneh, S. Liu, J. Li, *Int. J. Biol. Macromol.* 164 (2020) 2974-2986.
- [25] B. Ramalingam, M.M.R. Khan, B. Mondal, A.B. Mandal, S.K. Das, *ACS Sustainable Chem. Eng.* 3 (2015) 2291-2302.
- [26] M. Nikoorazm, P. Moradi, N. Noori, et al., *J Iran. Chem. Soc.*, 18 (2021) 467-478.
- [27] P. Moradi, M. Hajjami, *New J. Chem.*, 45 (2021) 2981-2994.
- [28] P. Moradi, M. Hajjami, *RSC Adv.*, 11 (2021) 25867-25879.
- [29] P. Moradi, M. Hajjami, *RSC Adv.*, 12 (2022) 13523-13534.
- [30] A. Ghorbani-Choghamarani, B. Tahmasbi, Z. Moradi, *Appl Organometal Chem.*, 31 (2017) e3665.
- [31] A. Ghorbani-Choghamarani, H. Rabiei, B. Tahmasbi, et al., *Res Chem Intermed*, 42 (2016) 5723-5737.
- [32] B. Tahmasbi, A. Ghorbani-Choghamarani, *New J. Chem.*, 43 (2019) 14485-14501.
- [33] B. Atashkar, A. Rostami, H. Gholami, et al., *Res Chem Intermed*, 41 (2015) 3675-3681
- [34] F. Rafiee, F. Rezaie Karder, *React. Funct. Polym.* 146, (2020) 104434.
- [35] F. Rafiee, F. Rezaie Karder, *Int. J. Biol. Macromol.* 146 (2020) 1124-1132.
- [36] F. Rafiee, S. Kermani, *Iran J. Sci. Technol. Trans Sci.* 45 (2021) 1631-1643.
- [37] A. Ananth, Y.S. Mok, *Nanomaterials* 6 (2016) 42.
- [38] T. Fang, D.M. Du, S.F. Lu, J. Xu, *Org. Lett.* 7 (2005) 2081-2084.
- [39] Z.B. Li, L. Pu, *Org. Lett.* 6 (2004) 1065-1068.
- [40] Z.C. Chen, X.P. Hui, C. Yin, L.N. Huang, P.F. Xu, X.X. Yu, S.Y. Cheng, *J. Mol. Catal. A. Chem.* 269 (2007) 179-182.
- [41] L.N. Huang, X.P. Hui, Z.C. Chen, C. Yin, P.F. Xu, X.X. Yu, S.Y. Cheng, *J. Mol. Catal. A. Chem.* 275 (2007) 9-13.
- [42] Y.F. Zhou, R. Wang, Z.Q. Xu, W.J. Yan, L. Liu, Y.F. Gao, C.S. Da, *Tetrahedron Asymm.*, 15 (2004) 589-591.